Available online at www.sciencedirect.com
SCIENCE DIRECT®
C. R. Physique 7 (2006) 163–169
COMPTES RENDUS PHYSIQUE
http://france.elsevier.com/direct/COMREN/

High power fiber lasers and amplifiers/Lasers et amplificateurs à fibre de puissance

Power limitation induced by nonlinear effects in pulsed high-power fiber amplifiers

Yves Jaouën [a,b,*], Guillaume Canat [b], Sébastien Grot [c], Sylvain Bordais [c]

[a] *GET/Telecom Paris, CNRS UMR 5141, 46, rue Barrault, 75634 Paris, France*
[b] *ONERA, DOTA/SLS, 2, chemin de la Hunière, 91761 Palaiseau, France*
[c] *Keopsys SA, 21, rue Louis de Broglie, 22300 Lannion, France*

Available online 3 March 2006

Abstract

The combining of double-clad (DC) doped fibers and semiconductor pump laser diodes has allowed the development of high power optical sources in CW or pulsed regimes. Compared to bulk medium, the main limitations for achieving high peak powers inside optical fibers are due to small mode field size and large propagation length. Nonlinear effects such as the optical Kerr effect, Stimulated Raman Scattering (SRS) or Stimulated Brillouin Scattering (SBS) can be observed in high power amplifiers as short as a few meters of doped fiber length. A description of the different non-linear dynamics for optical pulse amplification in dependence with temporal pulse duration (ps, ns and μs regimes) will be presented. Theoretical modelling has also investigated to confirm the observed signal distortions in the case of a ∼6 μm core doped fiber amplifier. The power increase requires the design of new doped fibers with a large core to enhance simultaneously stored energy and nonlinear effects threshold. The peak power threshold in dependence with temporal pulse duration (ps, ns and μs regimes) will be given in relation with core diameters of double-clad fibers. ***To cite this article: Y. Jaouën et al., C. R. Physique 7 (2006).***

Résumé

Limitations en puissance induites par les effets non-linéaires dans les amplificateurs à fibre en régime impulsionnel. La combinaison des technologies de fibres dopées double gaine et des diodes laser de pompe à semiconducteurs de forte puissance a permis le développement de sources optiques de forte puissance en régime continu ou pulsé. Les limitations principales pour atteindre les fortes puissances proviennent de la faible taille de mode dans le cœur de la fibre et de la grande longueur de propagation. Des effets non-linéaires de type Kerr optique, SRS (Stimulated Raman Scattering) ou SBS (Stimulated Brillouin Scattering) peuvent être observés dans les amplificateurs à fibre dopée de quelques mètres de longueur. Une description des différentes dynamiques non-linéaires en relation avec la durée des impulsions (régimes ps, ns et μs) sera présentée. De plus, des modèles théoriques permettront de confirmer les observations effectuées dans le cas d'amplificateurs à fibre dopée de ∼6 μm de diamètre de coeur. La montée en puissance requière la conception de nouvelles fibres à large cœur afin d'accroître simultanément l'énergie stockée et le seuil de puissance d'apparition des effets non-linéaires. Les seuils d'apparition des effets non-linéaires en terme de puissance crête seront donnés pour les différents régimes temporels en fonction des diamètres de cœur des fibres à double gaine. ***Pour citer cet article : Y. Jaouën et al., C. R. Physique 7 (2006).***

* Corresponding author.
E-mail address: yves.jaouen@enst.fr (Y. Jaouën).

1631-0705/$ – see front matter
doi:10.1016/j.crhy.2006.01.014

Keywords: Fiber amplifier; Double-clad fiber; Power amplifier; Erbium; Ytterbium; Non-linear effects

Mots-clés : Amplificateur à fibre ; Fibre à double gaine ; Amplificateur de puissance ; Erbium ; Ytterbium ; Effets non-linéaires

1. Introduction

In recent years, cladding-pumped fiber technology is of growing interest, with an increasing continuous-wave output power going from less than 1 W to more than 1 kW [1–4]. A double cladding fiber typically consists of a doped core (6–50 μm) for signal amplification, a large inner cladding (80–400 μm) which acts both as multimode waveguide for the pump light and as a cladding for the core, and an outer cladding to confine the pump in the inner cladding. Double-clad fibers with pure Yb^{3+} doping or Er^{3+}/Yb^{3+} co-doping are used to build efficient lasers at 1 and 1.55 μm respectively. A typical power amplifier consists in a MOPA (Master Oscillator – Power Amplifier) architecture as shown in Fig. 1. The first stage consists in a conventional core pump fiber amplifier with typical output power in 10-mW range. An isolator separating the 2 stages prevents the backward Amplifier Spontaneous Emission (ASE) from the power stage. A high input power is required to saturate the power amplifier stage. The moderate gain of the power stage limits the ASE generation. Different solutions have been proposed for pump injection in DC fibers such as V-groove side pumping technique or tapered fiber bundle [5].

Compared to bulk solid medium, the main limitations for achieving high peak powers in the fibers are due to small mode size and large propagation length. A simple comparison between typical mode sizes (MDF $\sim$ 6–10 μm versus 1–3 mm) and signal propagation lengths ($L \sim 3$–15 m versus 1–10 cm) in fiber and bulk solid medium, indicates that a fiber amplifier should be on the order of 10^5–10^6 times more sensitive to the peak-power induced nonlinear effects as compared to a solid-state amplifier. It is well-known that nonlinear effects such as the optical Kerr effect (SPM and OPA), SRS and SBS can be observed in silica fibers due to the long interaction length [6]. To analyse the induced nonlinear mechanisms, we have developed a numerical model based on the so-called generalized nonlinear Schrödinger equation (NLSE):

$$\frac{\partial A}{\partial z} = \underbrace{\sum_{k\geqslant 1} i^{k+1}\frac{\beta_k}{k!}\frac{\partial^k A}{\partial t^k}}_{\text{dispersion}} - \underbrace{\frac{g(z)}{2}}_{\text{gain}} A + \mathrm{i}\gamma\left(1+\frac{\mathrm{i}}{\omega_o}\frac{\partial}{\partial t}\right)\underbrace{\left[A(z,t)\int_{-\infty}^{t} R(t')\left|A(z,t-t')\right|^2 \mathrm{d}t'\right]}_{\text{nonlinear effects}} \tag{1}$$

Eq. (1) describes accurately the pulse propagation in fiber amplifiers for pulses as short as 50 fs and can be solved using a standard split-step Fourier method [6]. The γ parameter of Yb^{3+} doped and Er^{3+}/Yb^{3+} co-doped fibers has been determined using the FWM method [7]. Nonlinear coefficients $\gamma_{Yb} \sim 5$–$10\ W^{-1}\,km^{-1}$ and $\gamma_{ErYb} \sim 10$–$15\ W^{-1}\,km^{-1}$ have been measured in the case of standard $\sim$6 μm core double-clad fibers. The obtained values are 5–10 times higher compared to standard SMF fibers. The nonlinear coefficient is proportional to n_2/A_{eff}. We attribute the high values of γ parameters to an enhanced n_2 material Kerr coefficient due to the high co-doping concentration.

In this article, we focus on the influence of these nonlinear effects in high power fibre amplifiers as short as a few meters when the power-distance product is large. A description of the more significant nonlinear dynamics for optical pulse amplification will be presented. Indeed, theoretical modelling has been investigated to confirm the observed signal distortions for different high power amplifier configurations in the case of a $\sim$6 μm core doped fiber amplifier. Usually, the effective length of a passive fiber is defined as $L_{\text{eff}} = (1-\exp(-aL)/\alpha)$ [6] and corresponds a lossy fiber

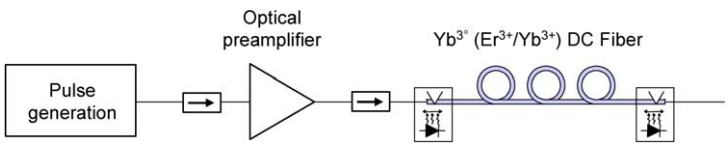

Fig. 1. Typical architecture of a high power Yb^{3+}(Er^{3+}/Yb^{3+}) doped fiber amplifier.

Fig. 1. Architecture typique d'un amplificateur à fibre dopée Yb^{3+} (Er^{3+}/Yb^{3+}) de puissance.

($L_{\text{eff}} < L$) where a similar level of nonlinear effects are induced. For a more simple approach in the case of a fiber amplifier, we propose an effective length related to output power defined as:

$$L_{\text{eff}} = \frac{1}{\exp gL} \cdot \int_0^L \exp(gz)\,\mathrm{d}z \tag{2}$$

Assuming uniform spatial gain distribution, (2) can be expressed as $L_{\text{eff}} = L(G-1)/G\log G$ where $G = \exp(gL)$. Counter-pumping is preferable to minimize effective length. Large-mode-area (LMA) fibers are required for extending the output powers and energies and enhancing the threshold powers of non-linear effects [8]. Different approaches have been proposed: low numerical aperture (NA) LMA single mode fiber (core diameter ∼12–15 μm), low NA slightly multimode fiber (core diameter 18–25 μm) and multimode mode fiber (core diameter 30–50 μm). A single mode amplification can be achieved using a multimode fiber by introducing strong loss of higher-modes: specific fiber coil configuration, optimized launch conditions of the input beam, specific cavity configurations. The peak power threshold dependence on temporal pulse duration (ps, ns and μs regimes) will be given in relation to core diameter.

2. Pulse amplification in ps regime

The propagation of short pulses in a high power fiber amplifier can be associated with severe distortions due to the Self Phase Modulation (SPM) effect (i.e., power variation induces frequency shift such as $\Delta\omega(t) = \gamma\,\mathrm{d}P/\mathrm{d}t\,L_{\text{eff}}$). SPM-induced pulse distortion has been investigated using a picosecond laser source and a 3.2 m Er^{3+}/Yb^{3+} fiber amplifier pumped in a contra-propagating arrangement [9]. Fig. 2(a) presents the output spectral broadening as a function of the output peak power. Strong spectral broadening is observed for output peak powers higher than 1 kW. Fig. 2(b) shows output spectrum at 4 kW peak power. The inset figure shows the amplifier spatial gain distribution that we used in the numerical modelling. The input pulse is assumed to be a 3.72 ps transform limited pulse, with 50 W peak power. The pulse wavelength broadening can be approximated as:

$$\Delta\omega_{\text{SMP}} \sim \gamma \frac{P_{\text{peak}}}{\tau} L_{\text{eff}} \tag{3}$$

Eq. (3) indicates that the maximum frequency broadening expected from SPM of pulses of 1 kW peak power and 10 ps duration is $\Delta\upsilon_{\text{SPM}} \sim 100$ GHz (i.e., $\Delta\lambda_{\text{SPM}} \sim 0.8$ nm). The CPA (Chirp Pulse Amplification) technique has been applied to obtain short optical pulses with high peak powers. In typical CPA architecture, the optical pulse can be stretched before amplification using highly dispersive fiber and then recompressed using a grating-pair compressor [9].

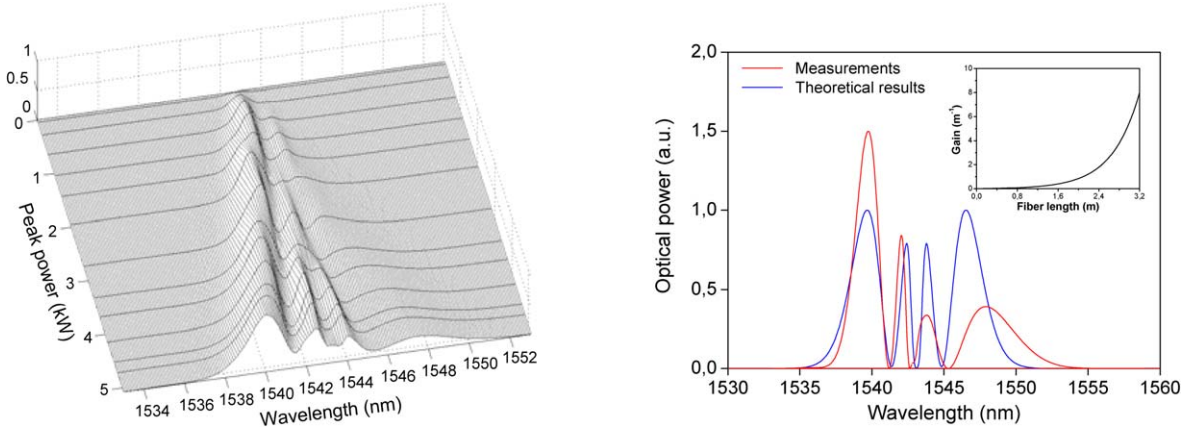

Fig. 2. Output Spectrum evolution of a 3.2 m counter-pumped Er^{3+}/Yb^{3+} amplifier ($\tau = 3.72$ ps) (a) peak power dependance, (b) modelling/measurements for output $P_{\text{peak}} = 4$ kW.

Fig. 2. Evolution du spectre de sortie d'un amplificateur Er^{3+}/Yb^{3+} de 3,2 m (P_{peak} d'entrée = 50 W, $\tau = 3.78$ ps) (a) en fonction de la puissance crête, (b) comparaison modélisation/mesures pour $P_{\text{peak}} = 4$ kW en sortie.

The use of bulk optics and gratings requires free space propagation and therefore needs complex optical alignment. Recently all-fiber CPA systems based on DCF (Dispersion Compensating Fiber) or chirped fiber grating stretcher combined with air-guiding photonic bandgap fiber compressor have been demonstrated [10,11].

3. Pulse amplification in ns regime

Other nonlinear phenomena, such as SRS and parametric four-wave mixing, contribute to the spectral broadening. The threshold power in relation with SRS effect that occurs in passive single-mode fibers can be approximated as [6]:

$$P_{\mathrm{SRS}} \sim 16\frac{A_{\mathrm{eff}}}{K g_{\mathrm{R}} L_{\mathrm{eff}}} \tag{4}$$

where g_{R} is Raman gain ($g_{\mathrm{R}} = 6.5 \times 10^{-14}$ m/W for pure silica) and K is the polarization dependance factor ($0.5 < K < 1$). The SRS wavelength shift generation has been analyzed using a 2 ns pulse source at 1064 nm that is injected in a pure Yb^{3+} fiber amplifier ($L = 7$ m, $\phi_{\mathrm{core}} \sim 6$ µm, co- and counter pumping architecture). The corresponding analytical SRS threshold power is $P_{\mathrm{SRS}} \sim 0.5$ kW. Fig. 3 presents output spectral evolution in dependance with output peak power. The 1st Raman Stoke peak is observed at 1115 nm (i.e., Raman frequency shift $\Omega_{\mathrm{SRS}} \sim 13.5$ THz). For low output peak power level, the 1st Raman profile corresponds to SRS generation in the pure silica output pigtail of 2 m length. Increasing the output peak power leads to the broadening of the 1st Stokes component and the generation of the 2nd Raman Stokes component at ∼1176 nm. Modelling shows good agreement with corresponding measurements. An analytic form was supposed for impulse Raman response [6,12].

It is well known that the Modulation Instability (MI) phenomenon (also so-called OPA effect) occurs in fiber with anormal dispersion propagation [6]. A parametric FWM process (nonlinear interaction between signal and noise) results in parametric gain g such as $g^2 = (\gamma P_{\mathrm{peak}})^2 - (\kappa/2)^2$ depending of phase matching parameter condition $\kappa = \Delta\beta + 2\gamma P_{\mathrm{peak}}$. No MI phenomenon is observed in monomode Yb^{3+} fiber amplifier because the chromatic dispersion is in normal regime (i.e., material dispersion $D_{\mathrm{m}} \sim -20$ ps/nm/km at 1064 nm) as shown in Fig. 3(a). The phase-matched parametric gain in Er^{3+}/Yb^{3+} fiber $g_{\mathrm{P}} = \gamma P_{\mathrm{peak}}$ is typically 10 times more compared to SRS gain $g_{\mathrm{SRS}} = g_{\mathrm{R}} P_{\mathrm{peak}}/A_{\mathrm{eff}}$ (i.e., assuming a output peak power $P_{\mathrm{peak}} = 1$ kW, $g_{\mathrm{P}} \sim 15$/m and $g_{\mathrm{SRS}} \sim 1.3$/m in case of ∼6 µm core Er^{3+}/Yb^{3+} fiber). Fig. 4(a) presents an output spectrum in the case of a 3 m Er^{3+}/Yb^{3+} fiber amplifier architecture. The corresponding numerical modelling have been obtained using launched signal with quantum noise limit condition level, $D = 15$ ps/nm/km and dominate counter-pumping. It is important to note that the enhanced OPA effect can be induced in LMA fibers in normal regime due to LP modes phase-matched parametric processes [13].

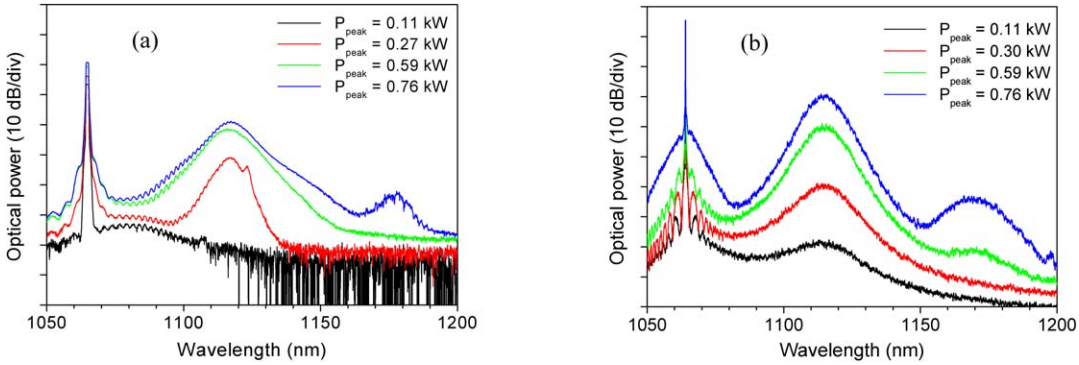

Fig. 3. Ouput spectra of a 6 m Yb^{3+} fiber amplifier for different output peak powers ($P_{\mathrm{in\ peak}} = 20$ W, $\tau = 2$ ns, $F_{\mathrm{rep}} = 3$ MHz): (a) measurements, (b) modelling results.

Fig. 3. Spectres de sortie d' un amplificateur à fibre Yb^{3+} de 6 m pour différentes puissances crêtes en sortie ($P_{\mathrm{in\ peak}} = 20$ W, $\tau = 2$ ns, $F_{\mathrm{rep}} = 3$ MHz) : (a) mesures, (b) modélisation numérique.

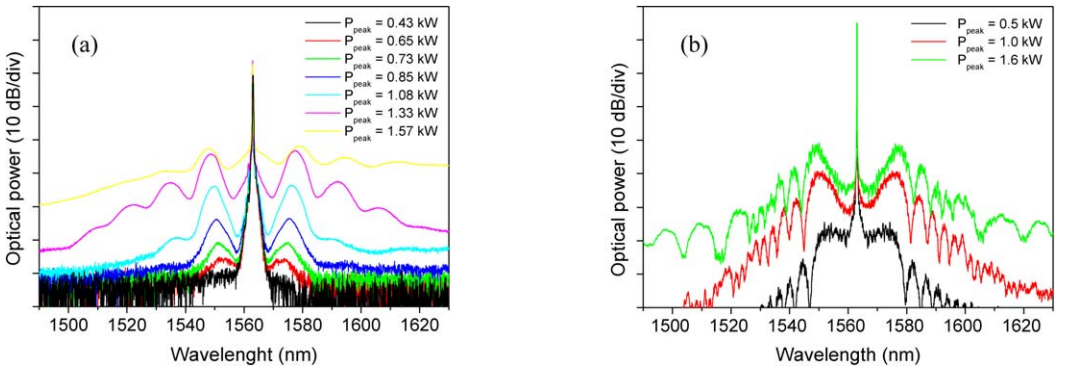

Fig. 4. Ouput spectra for a 3 m Er^{3+}/Yb^{3+} fiber amplifier for different output peak powers ($P_{\text{in peak}} = 50$ W, $\tau = 5$ ns, $F_{\text{rep}} = 80$ KHz: (a) measurements, (b) modelling results.

Fig. 4. Spectres de sortie d'un amplificateur Er^{3+}/Yb^{3+} de 3 m pour différentes puissances crêtes en sortie ($P_{\text{in peak}} = 50$ W, $\tau = 5$ ns, $F_{\text{rep}} = 80$ KHz : (a) mesures, (b) modélisation numérique.

4. Pulse amplification in µs regime

The dominant nonlinear effect for long pulse duration >10 ns is the SBS effect induced by spontaneous scattering of the incident pump wave. The threshold power which SBS occurs in passive single-mode fibers can be approximated as:

$$P_{\text{SBS}} \sim 21 \frac{A_{\text{eff}}}{K g_{\text{B}} L_{\text{eff}}} \tag{5}$$

where g_{B} is the Brillouin gain ($g_{\text{B}} = 5 \times 10^{-11}$ m/W for bulk silica and 2.5×10^{-11} m/W for SMF fiber [14]) and K is the polarization dependance factor ($1/3 < K < 2/3$ when $L_{\text{eff}} \gg L_{\text{B}}$ where L_{B} is the polarization beating length) [15]. We have measured Brillouin scattering in fiber amplifiers. The used SBS dynamic model is described in this issue by Canat's paper. To be consistent with theses measurements, modelling requires g_{B} values smaller one to two times smaller than SMF [16,17]. Fig. 5(a) presents output pulse distortion due to transient SBS in a 12 m Er^{3+}/Yb^{3+} fiber amplifier [18]. Cascaded Stokes lines generated by SBS are clearly observed. Only the even-order Stokes waves are co-propagating with the amplified input wave. The frequency spacing between the co-propagating Stokes lines is 0.17 nm (i.e., 2×10.6 GHz). The corresponding Brillouin frequency shift Ω_{B} is 10.83 GHz, in good agreement with the value measured in fused silica [6]. Fig. 5(b) shows the traces of output pulses corrupted by transient SBS. The pulse

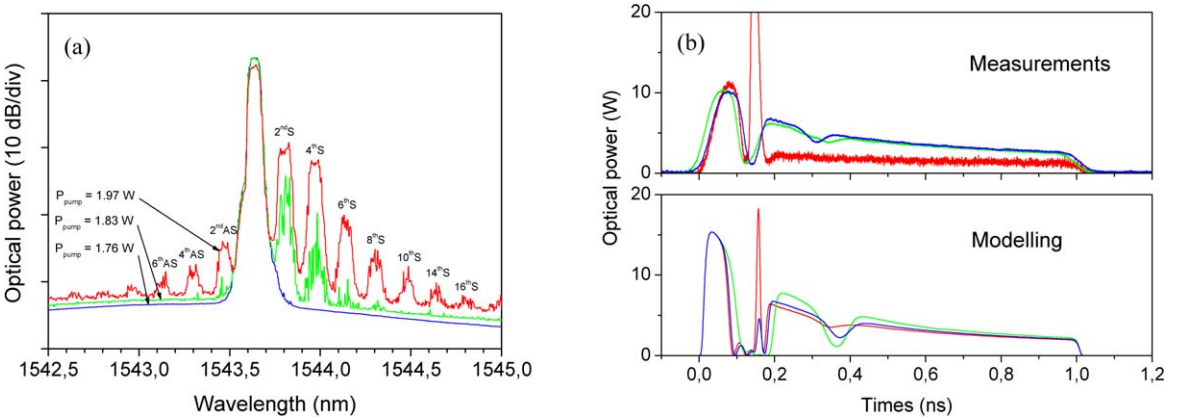

Fig. 5. Ouput spectra for a 12 m Er^{3+}/Yb^{3+} fiber amplifier for different output peak powers ($P_{\text{in peak}} = 0.2$ W, $\tau = 1$ µs: (a) multi-Stokes SBS spectrum, (b) temporal pulse evolution.

Fig. 5. Spectres de sortie d'un amplificateur à fibre Er^{3+}/Yb^{3+} de 12 m pour différentes puissances crêtes en sortie ($P_{\text{in peak}} = 0{,}2$ W, $\tau = 1$ µs : (a) spectres multi-Stokes, (b) évolution temporelle de l'impulsion.

Table 1
Power threshold in dependance with nonlinear effects

Tableau 1
Puissance de seuil en fonction des effets non-linéaires

Nonlinear effect origin		Pulse duration	Influence	Standard fiber $\phi_c \sim 6$ μm, NA ~ 0.12 $E_{max} \sim 10$–20 μJ	SM LMA fiber $\phi_c > 12$ μm, NA ~ 0.07 $E_{max} \sim 50$–100 μJ	MM LMA fiber $\phi_c > 20$ μm, NA ~ 0.07 $E_{max} \sim 0.1$–1 mJ
Kerr	SPM	<10 ps	Wavelength pulse broadening	0.5–2 kW	2–10 kW	>100 kW
	MI	10 ps – 10 ns	Energy out of pulse	0.5 kW	>5–10 kW	>20 kW
Scattering	Raman (SRS)	10 ps – 10 ns	wavelength range	∼0.5 kW	>5–10 kW	>20 kW
	Brillouin (SBS)	>10 ns	Temporal pulse distortion	10–30 W	50–120 W	>300 W

distortion is observed for output pulses >10 W. The stochastic aspect of SBS is initiated from spontaneous Brillouin scattering noise which results in a random fluctuation in output pulse shape. A dip in the instantaneous output power is observed at 0.12 μs after the rising edge of the pulse corresponding to a round trip time in the 12 m Er^{3+}/Yb^{3+} co-doped fiber. Considering the presence of optical gain along the Er^{3+}/Yb^{3+} co-doped fiber, a transient coupled-SBS equations model including an equation for the co-propagated 2nd Stokes wave has been proposed to analyze the distortion of the output pulses [18]. The amplifier gain dynamic has been modelled by an analytical saturation energy approach (Franz–Nodvick model). Recently, a more advanced theoretical model has been proposed that combines ions populations gain dynamic and non-linear effect dynamics, such as SBS, SRS and Kerr effects [19].

5. Conclusion

In this article, a description of pulse distortion induced by the different nonlinear effects occurring in high power fiber amplifiers has been presented. Good agreement between modelling and measurements in the case of small core diameter fibers ($\phi_{core} \sim 6$ μm) has been demonstrated. This modelling tool is very relevant for the optimization of fiber amplifier architectures (fiber length, pump and signal wavelengths dependance, pumping configuration, ...) and also to give guidelines for the design of new LMA doped fibers [19]. A double clad fiber with core diameter of ∼15 μm and NA ~ 0.07 is roughly the maximum that is compatible with single-mode propagation at 1.55 μm. As an example for LIDAR coherent applications, specific fiber amplifier architectures have been designed for >100 ns pulse amplification with narrow linewidth (<1 MHz) with no corruption of pulse shape by SBS effect: 0.1 mJ with $M^2 < 1.5$ using optimized amplifier chain architecture using commercial LMA fibers [16] and 0.29 mJ with $M^2 < 2.1$ with specifically designed fibers [20]. MM co-doped core fibers have been designed to deliver higher energy pulses (i.e., 1–10 mJ for $\phi_{core} \sim 20$–50 μm). Table 1 presents typical values of power threshold in dependance with the different nonlinear effects for different types of double-clad fibers (standard core diameter fibers, single-mode LMA fibers and MM LMA fibers).

References

[1] J. Limpert, CLEO'04, San-Francisco (2004), paper CMAA1.
[2] J. Nilsson, OFC'05, Anaheim (2005), paper OTuF1.
[3] J. Broeng, P.M.W. Skovgaard, J.R. Folkenberg, M.D. Nielsen, et al., PhotonicsWest'05, San Jose (2005), paper 5709-43.
[4] A. Tünnermann, A. Liem, PhotonicsWest'05, San Jose (2005), paper 5709-45.
[5] L. Golberg, G.M. Williams, J.-M. Delavaux, OFC'02, Anaheim (2002), paper WJ7.
[6] G.P. Agrawal, Non Linear Fiber Optics, Academic Press, San Diego, CA, 1989.
[7] Y. Jaouën, J.-P. Bouzinac, J.-M. Delavaux, C. Chabran, M. LeFlohic, Electron. Lett. 36 (2000) 233–235.
[8] J. Limpert, CLEO'04, SanFranscisco (2004), paper CMAA1.
[9] G. Kulscar, Y. Jaouën, E. Olmedo, M. Le Flohic, ECOC'91, Amsterdam (2001), paper We.L.3.4.
[10] J. Limpert, T. Schreiber, S. Nolte, H. Zellmer, A. Tünnermann, Opt. Express 11 (2003) 3332–3337.
[11] G. Imeshev, I. Hartk, M.E. Fermann, Opt. Express 12 (2004) 6508–6514.
[12] R.H. Stolen, C. Lee, R.K. Jain, J. Opt. Soc. Amer. B 1 (1984) 652–657.
[13] J. Dudley, L. Provino, N. Grossard, H. Maillotte, et al., J. Opt. Soc. Amer. B 19 (2002) 765–771.

[14] M. Nikles, L. Thevanaz, P.A. Robert, Lightwave Technol. 15 (1997) 1842–1851.
[15] M.O. van Deventer, A.J. Boot, Lightwave Technol. 12 (1994) 585–590.
[16] G. Canat, J.C. Mollier, J.-P. Bouzinac, Y. Aubry, G. Loas, Y. Jaouën, CLEO'05, Baltimore (2005), paper JWB67.
[17] G. Canat, A. Durecu, Y. Jaouën, S. Bordais, R. Lebref, CLEO'06, Long Beach (2006), submitted for publication.
[18] Y. Jaouën, G. Kulcsar, G. Canat, E. Olmedo, M. Le Flohic, OFC'03, Anaheim (2003), paper FB6.
[19] G. Canat, G. Williams, Y. Jaouën, J.-C. Mollier, B. Cole, et al., J. Opt. Soc. Amer. B 22 (2005) 2308–2318.
[20] V. Philippov, C. Codemard, Y. Jeong, C. Alegria, J.K. Sahu, J. Nilsson, G.N. Pearson, Opt. Lett. 29 (2004) 2590–2592.